Supplementary Information (SI) for ChemComm.
This journal is © The Royal Society of Chemistry 2024

Supplementary Information for

Separation of Rare Earth Elements and Nickel Harnessing Electrochemistry and Reactive CO_2 Capture and Mineralization

Prince Ochonma,[1] Akanksha Srivastava,[2] Christopher Noe,[3] Tianhe Yin,[2] Prarabdh Jain,[1] and Greeshma Gadikota[1,2,*]

[1]*Smith School of Chemical and Biomolecular Engineering, Cornell University, Ithaca, NY 14853*
[2]*School of Civil and Environmental Engineering, Cornell University, Ithaca, NY 14853*
[3]*Department of Chemistry, College of Art and Science, Stony Brook University, Stony Brook, NY 11790*

***Corresponding author:** Email: gg464@cornell.edu | Phone: 1-857-253-8724

Materials

Synthetic metal solutions are prepared with distilled and deionized 18 MΩ cm water using a Milli-Q system. Solutions bearing REE^{3+} and Ni^{2+} ions are prepared using lanthanum (III) chloride heptahydrate ($LaCl_3 \cdot 7H_2O$, purity 99%), neodymium (III) chloride hexahydrate ($NdCl_3 \cdot 6H_2O$, purity 99%), europium (III) chloride hexahydrate ($EuCl_3 \cdot 6H_2O$, purity 99%), dysprosium (III) chloride hexahydrate ($Dy(NO_3)_3 \cdot 6H_2O$, purity 99%), praseodymium (III) chloride heptahydrate ($PrCl_3 \cdot 7H_2O$, purity 99%) and nickel (II) chloride ($NiCl_2$, purity 98%), all purchased from Sigma Aldrich. Diethylenetriamine (DETA, Reagent Plus, purity 99%, Sigma Aldrich), monoethanolamine (MEA, laboratory grade, weight percent > 95%, Fisher Chemical) and ammonium hydroxide solution (25 % NH_3 in H_2O, Honeywell, and 28 % NH_3 in H_2O, Sigma-Aldrich) are used as liquid solvents. Electrolytes used for electrochemical measurements are sodium nitrate ($NaNO_3$, purity >99%). Ag/AgCl reference electrodes are purchased from Stony Lab (Nesconset, NY). Platinum sheet (10mm x 10 mm, thickness 0.1 mm, purity 99.99%) is used as the counter electrode. Titanium sheet (10 mm x 10 mm, thickness 0.25 mm, 99.7% trace metals basis) is used as the working electrode. Anion Exchange Membrane (AEM, Fumasep FAM) used for the bench-scale setup is a Celgard 3501 surfactant-coated porous polypropylene membrane.

Aqueous solutions used in REE separation experiments containing ~2.4 g/L of Ni with La to Ni ratios of 1:2, 1:1, and 2:1 is prepared by dissolving $LaCl_3 \cdot 7H_2O$ and $NiCl_2$ in de-ionized water. Subsequently the pH is adjusted to 6 to prevent any precipitation via hydrolysis.[1] Similarly, different REE and Ni solutions containing 2.4 g/L of Ni and REEs are prepared by dissolving $NdCl_3 \cdot 6H_2O$, $EuCl_3 \cdot 6H_2O$, $Dy(NO_3)_3 \cdot 6H_2O$, $PrCl_3 \cdot 7H_2O$, and $NiCl_2$ in de-ionized water. Control experiments are performed by directly bubbling CO_2 into the metal bearing solution and using CO_2 loaded NaOH. The effectiveness of regenerable solvents such as NH_4OH, MEA and DETA in facilitating the recovery of REE carbonates is investigated. 20 ml of 0.5 M CO_2 loaded NH_4OH, MEA or DETA is added to 20 ml of the solution bearing metals. The resulting solution containing 0.25 M CO_2 loaded NH_4OH, MEA or DETA and 1.2 g/L of Ni in different Ni: REEs is then reacted for 60 minutes. The CO_2 loaded solvent is obtained by bubbling 10% CO_2 gas mixture through the solvent for ~ 12 hours. Solid precipitates are then collected via centrifugation and dried in an oven for further characterization.

Electrodeposition Measurements

All electrochemical measurements are performed with a potentiostat (Interface 1010E, Gamry Instruments) in a H-Type Electrolytic Cell using a 3-electrode system. The working electrode (cathode) is a piece of titanium sheet with an area of 1 × 1 cm^2 (thickness of 0.25 mm). The reference and counter (anode) electrodes are Ag/AgCl electrode and a platinum sheet with an area of 1 × 1 cm^2 (thickness of ~ 0.1 mm), respectively. All potentials in this work are in reference to Ag/AgCl unless otherwise specified. Electrodeposition experiments are performed in three distinct modes. Mode 1 represents the base case experiments to elucidate the effect of solvents in this recovery process. These base case electrochemical measurements are performed using 40 ml of 1.2 g/L Ni solution and 0.25 M of solvents of either NH_4OH, MEA or DETA as the catholyte. In mode 2, the solution bearing nickel, and the solvent are first contacted with 10% CO_2 for 2 hours prior to electrochemical measurements. The hypothesis that the formation of carbamate could facilitate ease of Ni deposition is tested in this mode. In mode 3, CO_2 is bubbled through the catholyte solution during electrochemical measurements. All experiments for alkaline electrolysis are performed using 40 ml of 0.25 M $NaNO_3$ as the anolyte. All experiments are conducted at room temperature. To investigate the influence of CO_2 on electrodeposition, the gas containing 10% CO_2 is supplied continuously at 1 atm to the catholyte during electrodeposition.

Product Characterization

Solid and liquid samples are obtained for every experiment after separation and decantation using a centrifuge. The recovered solid is washed with deionized water and then dried in an oven at 100 (±3) ^oC for 12 hours, while known amounts of the recovered liquid are prepared for further analysis by dilution with 5 wt.% nitric acid. To determine the quantitative efficiencies of these experiments, concentrations of metal cations in the liquid solutions before and after experiments are determined via Inductively Coupled Plasma - Optical Emission Spectroscopy (ICP-OES). The recovery efficiencies, separation factor, and purity of the recovered solid are determined using the **Equations 1 - 4** below.

$$\eta_{mi} = \frac{C_{mi} * V_m - C_{ji} * V_j}{C_{mi} * V_m} * 100 \quad (1)$$

$$P_{mi} = \frac{C_{mi} * V_m - C_{ji} * V_j}{\sum_{i=1}^{k} (C_{mi} * V_m - C_{ji} * V_j)} * 100 \quad (2)$$

$$\beta = \frac{D_{mi}}{D_{mj}} \quad (3)$$

$$D_m = \frac{C_c}{C_s} \quad (4)$$

In the equations above, η_{mi} is the recovery efficiency of metal "i" measured in %, P_{mi} is the purity of metal "i" carbonate product, and the separation factor is defined as β. C_{mi} and C_{ji} are the concentration of metal "i" in solution before (m) and after (j) either CO_2 mineralization or electrodeposition experiments respectively, and C_c and C_s are the moles of metal in the carbonate and in the solution phase, respectively. V_m and V_j represent the volume of the solutions before and after the experiments respectively, D_i and D_j compare the affinity of a metal M in each phase as either carbonate or soluble complex, and k is the total number of metals dissolved in solution at the start of the experiment. The quantification and speciation of CO_2 in the different solvents including NH_4OH, MEA, and DETA are investigated using ^{13}C Nuclear Magnetic Resonance (NMR) and Fourier Transformed Infrared (FTIR) spectroscopy. NMR data are acquired on a 500 MHz Bruker AVIII spectrometer equipped with a Prodigy BBO probehead. 13C spectra are acquired with 1024 scans, 30 seconds relaxation delay, 32.5 kHz spectral width, and 1.5 s acquisition time. The spectra are processed in MNova (version 14.2.3, Mestrelab Research S.L.). The FIDs are zero filled to 128k points prior to Fourier transform. Automatic phase correction is applied followed by baseline correction with 7th-order Bernstein polynomials. Spectra are superimposed and the frequencies are aligned using solute signals and integrated using automatic linear correction for solute signals.

The dried solids are weighed and characterized further. The release of volatile components resulting in changes in the sample weight and thermal decomposition behavior of carbonate products are determined using a Thermogravimetric Analyzer (TGA, Discovery SDT 650, TA instrument). The samples are heated from room temperature to 1000 ˚C at a ramp rate of 5 °C/min under a constant N_2 flow rate (50 mL/min). The crystalline phases of the carbonate product and electrodeposited nickel are determined using X-ray Diffraction (XRD) (X-ray diffractometer, Bruker D8 Advance ECO powder diffractometer) with Cu Kα radiation (40 kV, 25 mA). The

samples are scanned over the 2θ range from 20˚ to 80˚. The obtained data are analyzed by Jade software, and crystalline species are identified by the International Centre for Diffraction Data (ICDD) database. The chemical bonding and functional groups in the synthesized products are evaluated using FTIR, acquired in an Attenuated Total Reflection (ATR) mode using an Attenuated Total Reflection-Fourier Transform Infrared spectrometer (ATR-FTIR, Nicolet™ iS50, Waltham, MA). Finally, the morphologies of these samples are observed using a Scanning Electron Microscope (SEM, Zeiss LEO 1550 FESEM). X-ray photoelectron spectroscopy (XPS) survey scans are used to examine the chemical states and surface compositions of the products. The CasaXPS curve resolution platform is used to analyze the peaks of interest using a combination of 30/70% Lorentzian/Gaussian functions, along with a Shirley or Tougaard background. These measurements together provide detailed insights into the chemical and morphological characteristics of the REE carbonate products, and electrodeposited Ni recovered during CO_2-assisted metal separation and recovery.

Coulombic Efficiency Calculations

$$\eta_C = m/M \quad (5)$$

The nickel current/coulombic efficiency (η_C) was calculated using the **equation 5**, where m is the experimental mass of nickel deposited on the surface of the titanium electrode, and M is the theoretical mass calculated by considering all the charge supplied for the nickel reduction process.

In this study Titanium sheet was used to electrodeposit nickel. Platinum and glassy carbon electrodes have been reported to have a higher activity for hydrogen evolution as well as nickel reduction compared to the titanium electrode.[2] However these materials are expensive for scale up considerations. Furthermore, it has been reported that titanium shows good resistance to the presence of chloride ions.[3]

Table S.1: REE and Nickel recovery efficiencies in carbonate product and La product purity for REEs and Nickel separation measurements. The starting concentration of Nickel is constant (2.4 g/L) for all experiments while REE concentrations are varied depending on the REE to Ni ratios. 1:2, 1:1 and 2:1 represent 1.2 g/L REE: 2.4 g/L Ni, 2.4 g/L REE: 2.4 g/L Ni, 4.8 g/L REE: 2.4 g/L Ni respectively. All experiments are carried out under atmospheric conditions (25^{o}C, 1 bar). * shown in separation factor represents the lowest values obtained in cases where the highest values are indeterminate (∞) as a result of zero nickel distribution.

Experimental	REE Recovery Efficiency [Nickel co-recovered] (%)	Lanthanum Product Purity (%)	Separation Factor (β)
Deionized water + Solution bearing La and Ni (1:2)	0 [0]	0 [0]	0 [0]
CO_2 bearing NaOH solvent + Solution bearing La and Ni (1:2)	99.89 (± 0.1) [70.73 (± 0.5)]	46.37 (± 0.7)	370.48 (± 8.21)
CO_2 bearing NH_4OH solvent + Solution bearing La and Ni (1:2)	99.86 (± 0.04) [14.64 (± 2.13)]	79.86 (± 2.24)	4523.9 (± 635.9)
CO_2 bearing NH_4OH solvent + Solution bearing La and Ni (1:1)	99.94 (± 0.005) [16.86 (± 0.63)]	83.45 (± 3.57)	8405.3 (± 291)
CO_2 bearing NH_4OH solvent + Solution bearing La and Ni (2:1)	99.96 (± 0.0006) [18.97 (± 1.9)]	91.22 (± 2.13)	11629.7 (± 1437)
CO_2 bearing MEA solvent + Solution bearing La and Ni (1:2)	99.76 (± 0.02) [16.43 (± 1.1)]	77.32 (± 0.43)	2131.5 (± 35.7)
CO_2 bearing MEA solvent + Solution bearing La and Ni (1:1)	99.9 (± 0.0006) [31.27 (± 2.53)]	79.26 (± 1.74)	3620 (± 8.1)
CO_2 bearing MEA solvent + Solution bearing La and Ni (2:1)	99.82 (± 0.15) [35.21 (± 2.97)]	85.52 (± 3.85)	4456.7 (± 637.4)
CO_2 bearing DETA solvent + Solution bearing La and Ni (1:2)	99.53 (± 0.07) [0.78 (± 0.78)]	98.23 (± 1.77)	11052*

CO_2 bearing DETA solvent + Solution bearing La and Ni (1:1)	99.62 (± 0.02) [2.76 (± 2.76)]	99.19 (± 0.81)	9145*
CO_2 bearing DETA solvent + Solution bearing La and Ni (2:1)	99.78 (± 0.01) [2.73 (± 2.73]	98.61 (± 1.39)	8784*
CO_2 bearing NH_4OH solvent + Solution bearing Nd and Ni (1:2)	99.94 (± 0.04) [42.14 (± 6.63)]	57.61 (± 1.37)	11793
CO_2 bearing NH_4OH solvent + Solution bearing Pr and Ni (1:2)	99.92 (± 0.02) [42.97 (± 6.55)]	58.14 (± 2.71)	3184.7
CO_2 bearing NH_4OH solvent + Solution bearing Dy and Ni (1:2)	99.77 (± 0.03) [25.01 (± 19.25)]	73.82 (± 17.36)	6239.1
CO_2 bearing NH_4OH solvent + Solution bearing Eu and Ni (1:2)	97.54 (± 2.32) [10.45 (± 2.55]	85.05 (± 3.36)	8818.34

Table S.2: Stability Constants for possible complexes formed by Nickel and REE species with the solvents used (NH_4OH, MEA and DETA) and CO_2 species.

Metal ion (M)	Complexing ion/solution (L)	Equilibrium (s = solid)	Log K	Temperature (°C) [Ionic Strength]	Source
Ni^{2+}	NH_4OH	ML	2.72 – 2.85	25[0 – 0.5]	[4]
Ni^{2+}	NH_4OH	ML_2	4.89 – 5.14	25[0 – 0.5]	[4]
Ni^{2+}	NH_4OH	ML_3	6.55 – 6.92	25[0 – 0.5]	[4]
Ni^{2+}	NH_4OH	ML_4	7.67 – 8.17	25[0 – 0.5]	[4]
Ni^{2+}	NH_4OH	ML_5	8.34 – 8.95	25[0 – 0.5]	[4]
Ni^{2+}	NH_4OH	ML_6	8.31 – 9.12	25[0 – 0.5]	[4]
Ni^{2+}	MEA	ML	2.98 – 3.06	25[0.1 – 0.5]	[5]
Ni^{2+}	MEA	ML_2	5.33 – 5.52	25[0.1 – 0.5]	[5]
Ni^{2+}	MEA	ML_3	6.95 – 7.33	25[0.1 – 0.5]	[5]
Ni^{2+}	DETA	ML	10.5	25[0.1]	[5]
Ni^{2+}	DETA	ML_2	18.6	25[0.1]	[5]
Ni^{2+}	CO_3^{2-}	ML	3.57	25[0.7]	[6]
Ni^{2+}	CO_3^{2-}	ML(s)	-6.87	25[0]	[4]
La^{3+}	CO_3^{2-}	M_2L_3 (s)	-33.4	25[0]	[4]
Nd^{3+}	CO_3^{2-}	M_2L_3 (s)	-33.0	25[0]	[4]
Dy^{3+}	CO_3^{2-}	M_2L_3 (s)	-31.5	25[0]	[4]
Eu^{3+}	CO_3^{2-}	M_2L_3 (s)	-32.3	25[0]	[7]

1

2

Table S.3: Possible Reaction pathways for REE-MEA-CO_2-H_2O system.

Phenomena	Reactions	Refs
Water dissociation	$H_2O_{(l)} \rightarrow H^+_{(aq)} + OH^-_{(aq)}$	8
CO_2 hydration	$CO_{2(aq)} + H_2O_{(l)} \rightarrow H_2CO_3{}^*_{(aq)}$	8
	$H_2CO_3{}^*_{(aq)} \rightarrow HCO_3{}^-_{(aq)} + H^+_{(aq)}$	8
	$HCO_3{}^-_{(aq)} \rightarrow CO_3{}^{2-}_{(aq)} + H^+_{(aq)}$	8
Carbamate Formation	$HCO_3{}^-_{(aq)} + H_2NC_2H_4OH_{(aq)} \rightarrow HOC_2H_4NHCOO^-_{(aq)} + H_2O_{(l)}$	8,9
	$CO_3{}^{2-}_{(aq)} + H^+_{(aq)} + H_2NC_2H_4OH_{(aq)} \rightarrow HOC_2H_4NHCOO^-_{(aq)} + H_2O_{(l)}$	9
	$HOC_2H_4NHCOO^- + H^+_{(aq)} + H_2O_{(l)} \rightarrow HCO_3{}^-_{(aq)} + HOC_2H_4NH_2H^+_{(aq)}$	9
REE Carbonate Formation	$2REE^{3+}_{(aq)} + 3HCO_3{}^-_{(aq)} \rightarrow REE_2(CO_3)_{3(s)} + 3H^+_{(aq)}$	
	$2REE^{3+}_{(aq)} + 3CO_3{}^-_{(aq)} \rightarrow REE_2(CO_3)_{3(s)}$	
	$HOC_2H_4NHCOO^-_{(aq)} + REE^{3+}_{(aq)} \rightarrow REE(HOC_2H_4NHCOO^-)_{3(aq)}$	
MEA Regeneration	$2REE(HOC_2H_4NHCOO^-)_{3(aq)} + 9H^+_{(aq)} \rightarrow REE_2(CO_3)_{3(s)} + 6H_2NC_2H_4OH_{(aq)} + 3HCO_3{}^-_{(aq)}$	

REE is an abbreviation for Rare Earth Elements including La, Pr, Dy, Nd, and Eu used in this study.

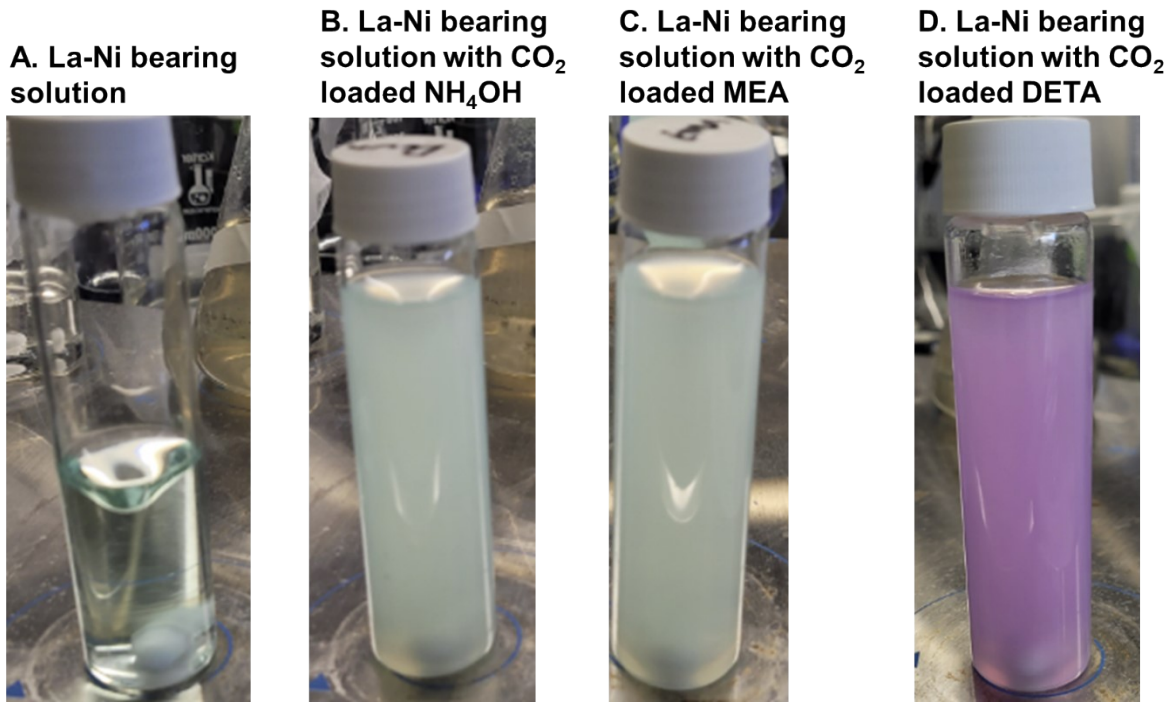

Fig. S.1: Snapshot showing **(a)** Lanthanum and Nickel bearing solution before reaction with solvents. Snapshot of Lanthanum and Nickel bearing solution during reaction with CO_2 loaded solvents including **(b)** NH_4OH, **(c)** MEA, and **(d)** DETA.

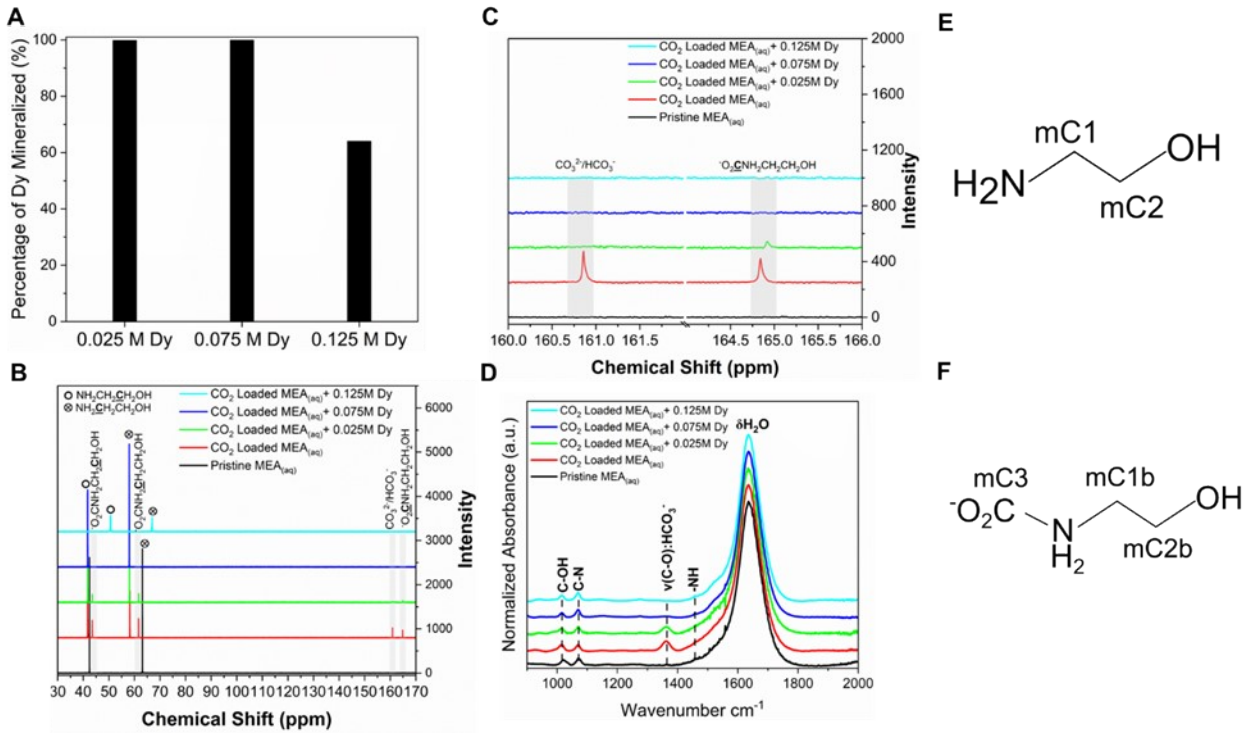

Fig. S.2: Solvent regeneration experiments with aqueous CO_2 loaded Monoethanolamine (MEA) using various concentrations of solution bearing Dysprosium (Dy). All experiments were carried out at room temperature for 1 hour. a) Extent of CO_2 mineralization as Dy carbonate as a function of increasing Dy concentration. b) FTIR spectra showing aqueous solvent transformations before CO_2 loading (pristine MEA at 0.25M) , after CO_2 loading, after reaction with 0.025 M Dy in solution, after reaction with 0.075 M Dy in solution, and after reaction with 0.125 M Dy in solution. c) ^{13}C NMR spectrum of solution transformations before CO_2 loading (pristine MEA at 0.25M) , after CO_2 loading, after reaction with 0.025 M Dy in solution, after reaction with 0.075 M Dy in solution, and after reaction with 0.125 M Dy in solution. d) Inset of (c) showing the formation and disappearance of carbamate and bicarbonate ions during CO_2 loading and with increasing Dy concentrations respectively. e) The structure and labeled carbon nuclei for MEA, and f) The structure and labeled carbon nuclei for $MEACOO^-$ See Table S.3 for possible reactions associated with these transformations.

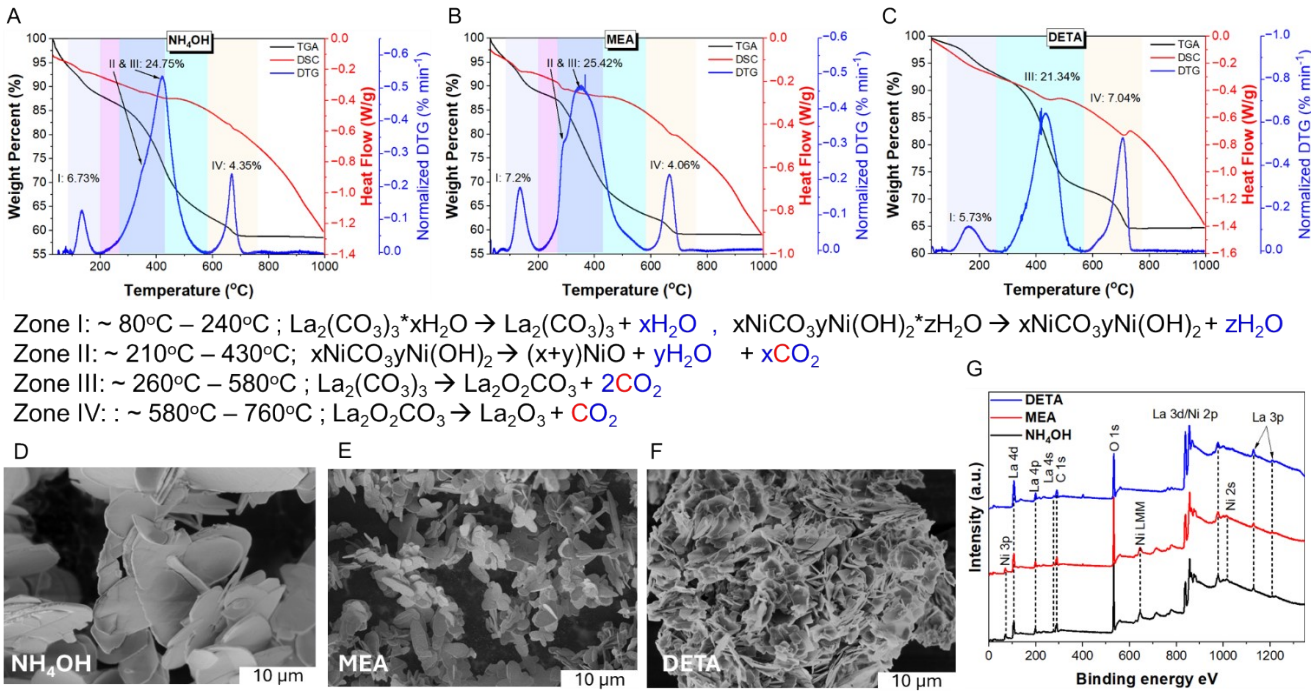

Fig. S.3. Evidence of carbonate formation based on TGA analyses of the product obtained by using **(a)** NH_4OH, **(b)** MEA, and **(c)** DETA. Detailed reactions showing the release of volatile components, and their associated temperature ranges are outlined. SEM images showing the rosette and flat like morphologies of carbonate products obtained post La separation using **(d)** NH_4OH, **(e)** MEA, and **(f)** DETA. XPS survey scans show the elemental distribution of the product for all cases in **(h)**. Rosette and flat morphologies in all lanthanum carbonate samples produced is consistent with prior published results[10]

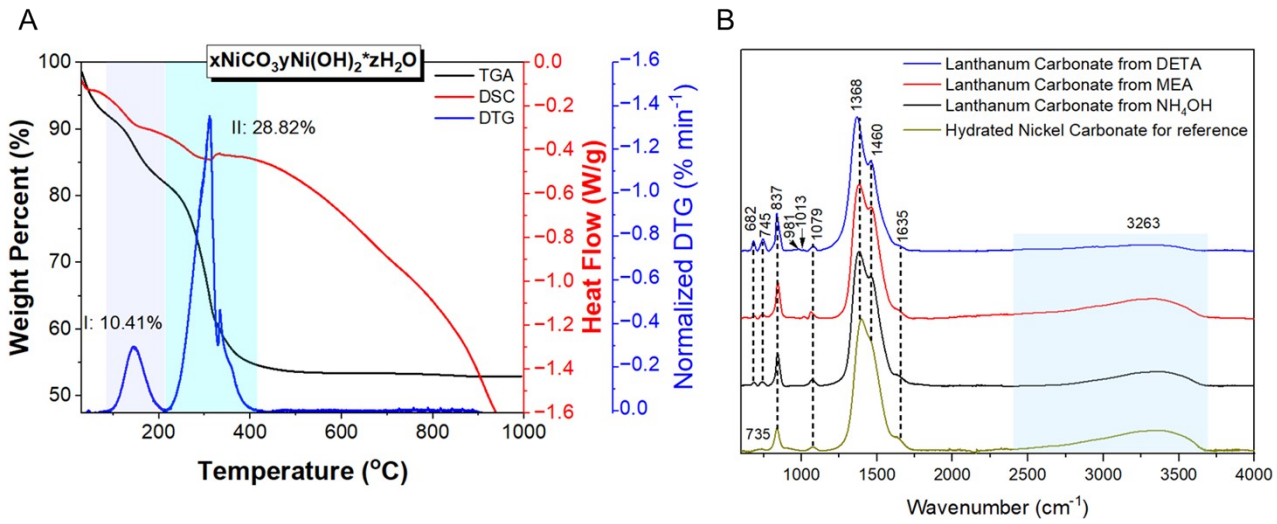

Fig. S.4: **(a)** Decomposition behavior of nickel carbonate is evident from TGA, DTG and DSC curves. **(b)** The bonding states obtained for carbonate products obtained using NH_4OH, MEA and DETA as solvents are shown in the FTIR spectra. Evidence of $Ni(OH)_2$ formation is observed with the absence of OH stretching peak at wavenumber of 3645 (± 3) cm [11,12]

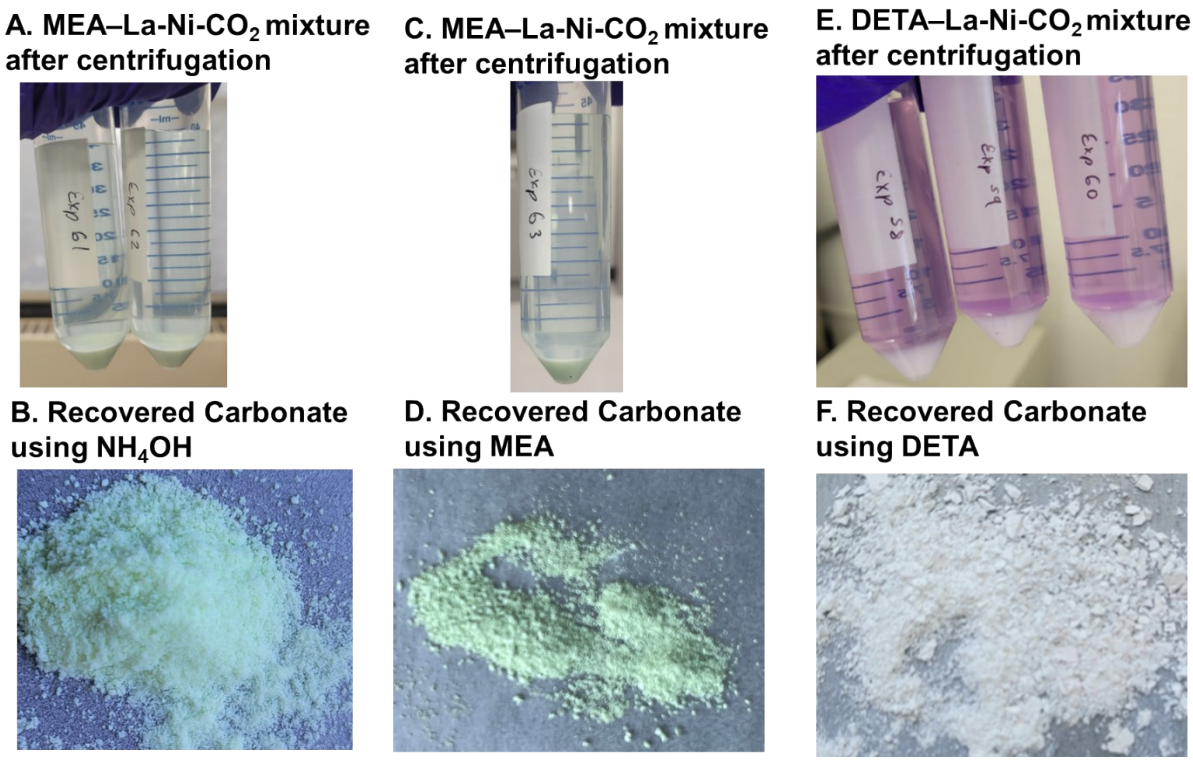

Fig. S.5: Snapshot of product slurry after centrifugation for NH_4OH, MEA and DETA are shown in (a), (c), and (e), respectively. Dried product recovered for analysis using NH_4OH, MEA, and DETA is shown in (b), (d), and (f), respectively.

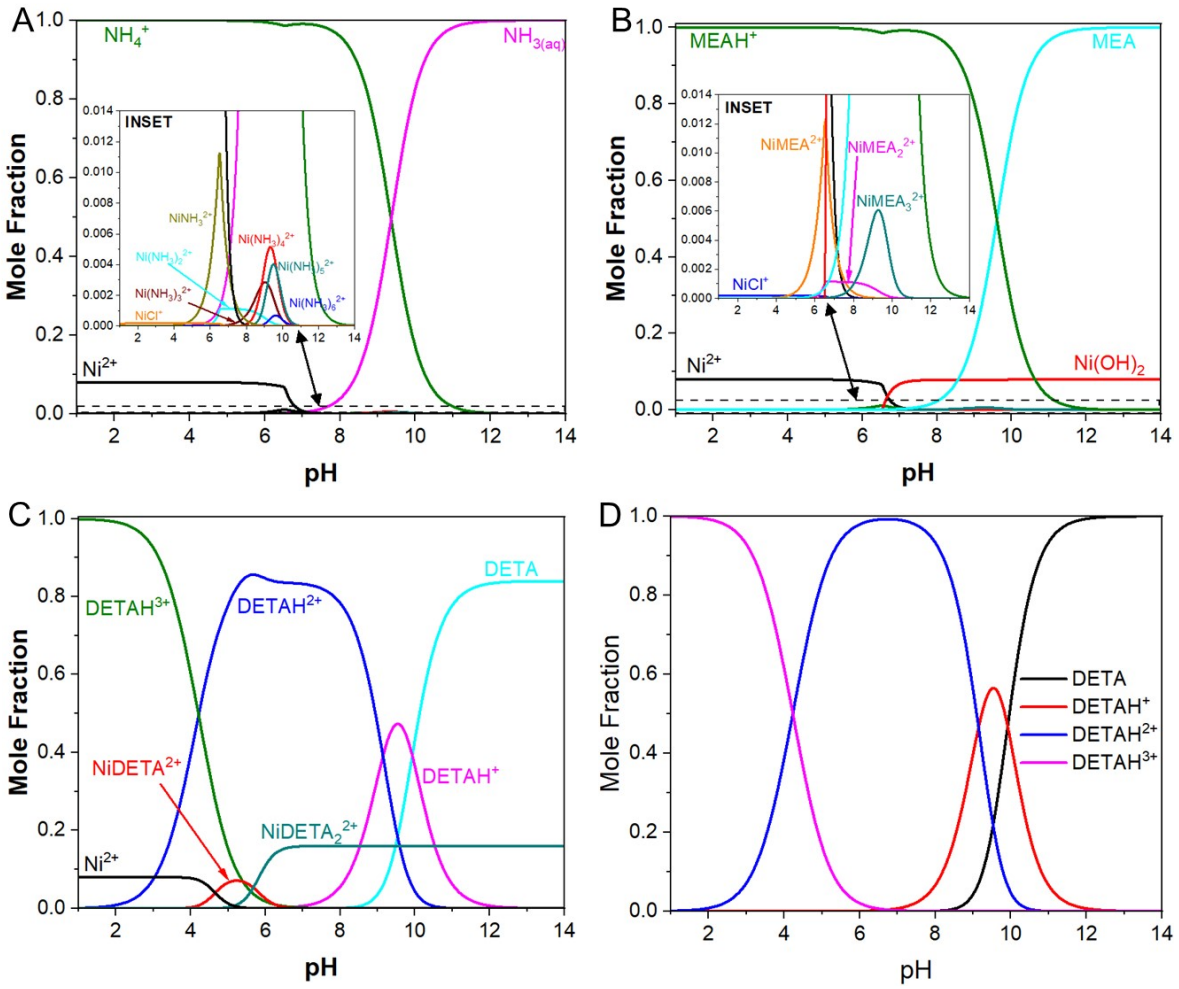

Fig. S.6: Speciation of Ni in the presence of **(a)** NH_4OH, **(b)** MEA and **(c)** DETA speciation in water as a function of pH is shown. DETA speciation in water as a function of pH is shown in **(d)**.

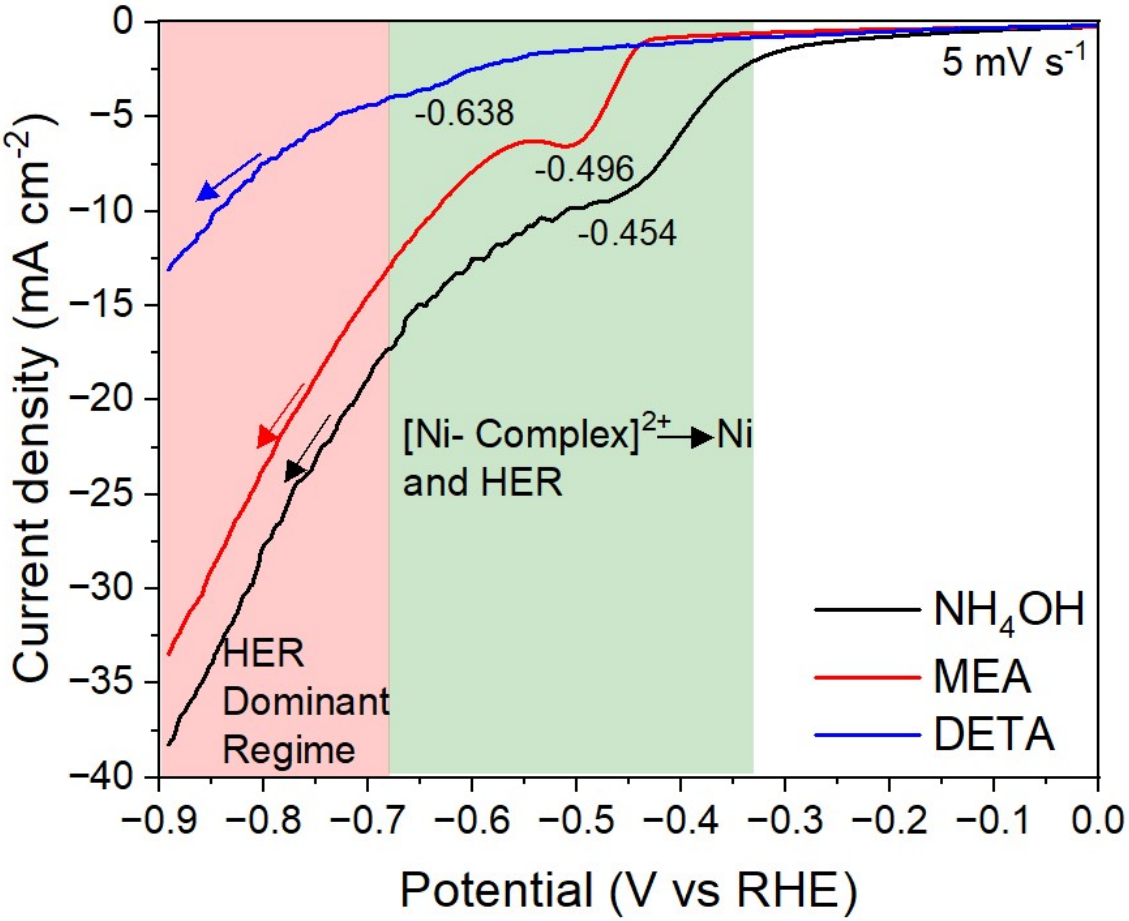

Fig. S.7. LSV curves of Titanium electrode surface is shown in different solvents with scanning rate of 5 mVs^{-1}

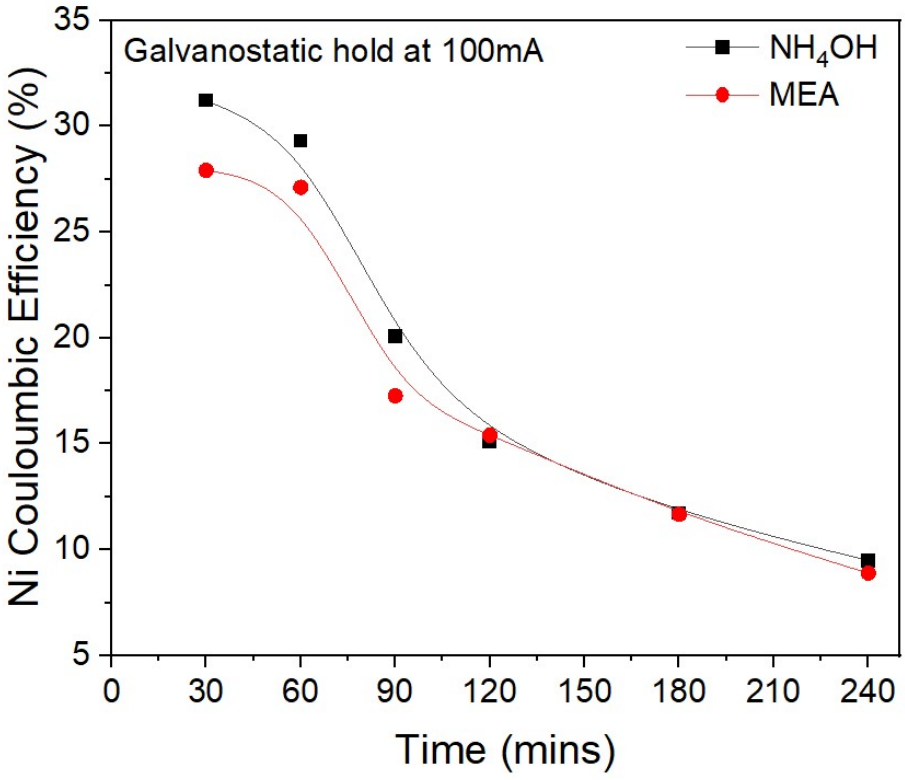

Fig. S.8: Ni coulombic efficiency as a function of time using 1.2 g/L of nickel in NH_4OH and MEA solvents.

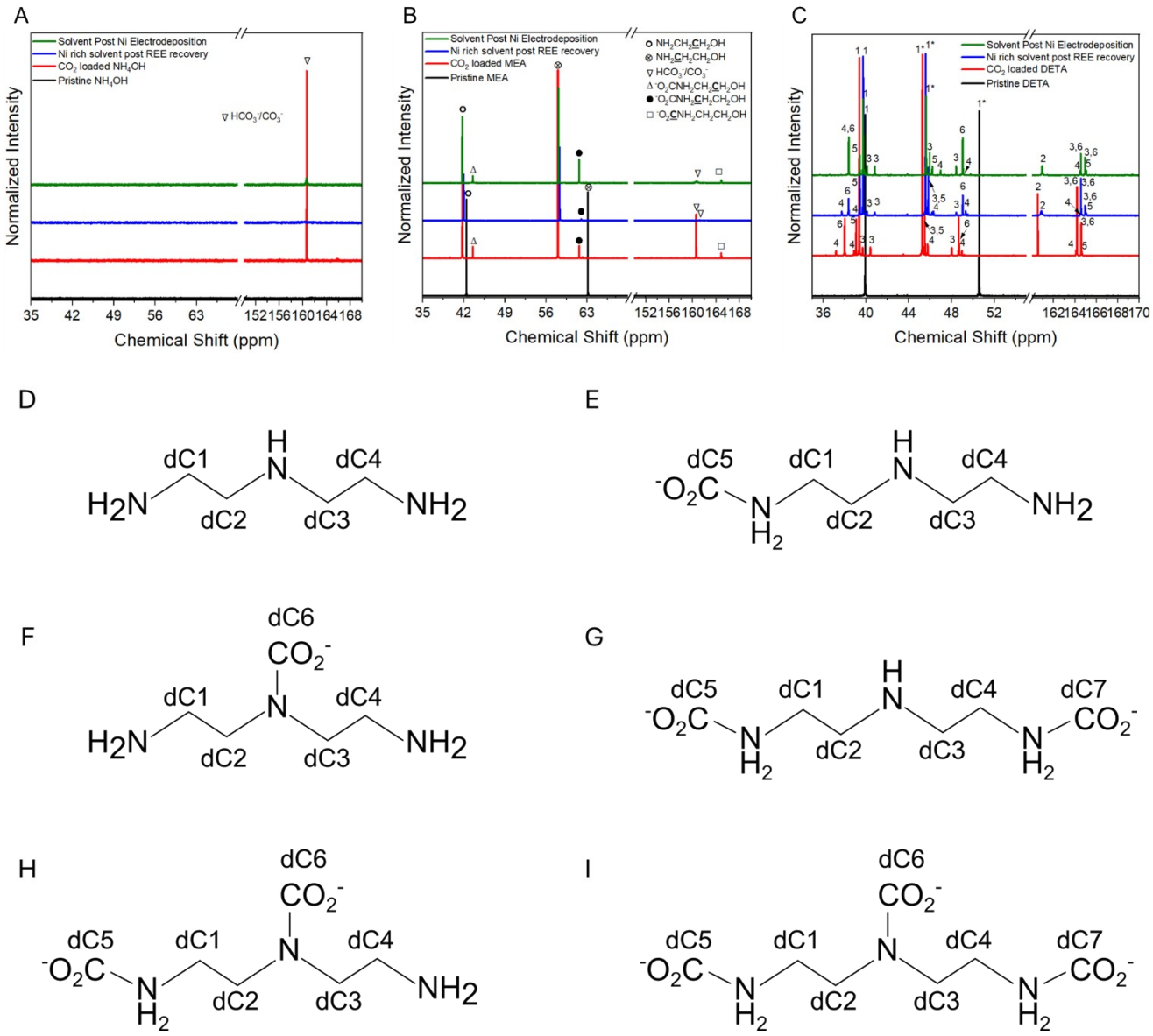

Fig. S.9: ^{13}C NMR spectrum of pristine solvent, CO_2 loaded solvent, solvent post REE separation and solvent after electrodeposition in **(a)** NH_4OH, **(b)** MEA, and **(c)** DETA solvents. Labelling in **(c)** 1/1* - Free DETA [$_2HN(CH_2)_2NH(CH_2)_2NH_2$], 2 – Bicarbonate/Carbonate [HCO_3^-/ CO_3^-], 3-Carbamate for single CO_2 on either side of the primary amine , 4- Carbamate for two CO_2 on a primary and secondary amine, 5- Secondary carbamate for single CO_2 on secondary amine, and 6 - Carbamate for two CO_2 on primary amines is shown. No decomposition or dissociation of solvent is observed using the proposed approach. This is also in agreement with FTIR analysis shown in **Fig S. 13.** It is important to note that the NMR spectra for solvent post Ni electrodeposition was done for the case where 10% CO_2 was also bubbled during electrodeposition experiments. **(e-i)** Structural representation of the various carbamate species that can form during the CO_2 loading of DETA.

NMR Analysis of Fig S. 9

For NH_4OH, only carbonate/bicarbonate species were observed using ^{13}C NMR which completely disappears with the introduction of solution bearing Lanthanum and reappears during electrochemical recovery of nickel from solution with simultaneous CO_2 bubbling.

Free, unreacted MEA features 2 peaks in its 13C NMR spectrum, corresponding to each of its 2 carbon nuclei, mC1 and mC2 (See Fig. S.2 e). MEA-carbamates feature a shift in these two peaks, making the formation of MEACOO- easily discernible by the appearance of a second set of peaks, corresponding to carbons mC1b and mC2b along with the carbamate carbon, mC3 (Fig. S.2f). The $MEAH^+$ expected to form via Table S.3 does not have NMR peaks discernible from those of unreacted MEA.[13] In these experiments, the formation of MEA-carbamates is observed during CO2 loading via bubbling. Following the introduction of nickel/lanthanum-bearing solution for the recovery of lanthanum carbonates, the peaks associated with MEA-carbonates/carbamate are either reduced or no longer present, suggesting their consumption in the process. The electrochemical recovery of nickel from solution with simultaneous CO_2 bubbling regenerates MEA-carbamates, as is shown by the reemergence of peaks mC3, mC1b, and mC2b.

Due to its symmetry, free DETA exhibits only 2 ^{13}C NMR peaks. However, DETA features 3 amine sites for carbamate formation, resulting in a variety of carbamate species apparent in the degree of peak splitting observed in the ^{13}C NMRs of DETA solution following CO_2 loading (Fig. S.9b). CO_2 loading results in the splitting of DETA's two peaks into a collection of smaller peaks (Fig. S.9b), indicative of the variety of carbamate species forming during the loading process. The dominance of the free DETA peaks suggest that it remains the main DETA species in solution. Following the recovery of lanthanum via precipitation, a decrease in all carbamate peaks is observed, though not to the extent that is observed with MEA. The most notable decrease is seen in the CO_3^{2-}/HCO_3^- peak, in this case attributed to HCO_3^- due to its position between 160.5-161.0ppm. As expected, pure DETA exhibits a clear lack of peaks in the range of 160ppm-166ppm (Fig. S.9b). Following CO_2 loading, a strong HCO_3^- peak is observed, along with the various carbamate peaks expected of highly loaded DETA.[14] It is also of interest to note that following electrochemical recovery of nickel, carbamate peaks were seen to make stronger resurgence than the HCO_3^- peak (Fig. S.9b), indicating that CO_2 loading during electrochemical recovery of nickel encourages the capturing of CO_2 in the form of carbamate.

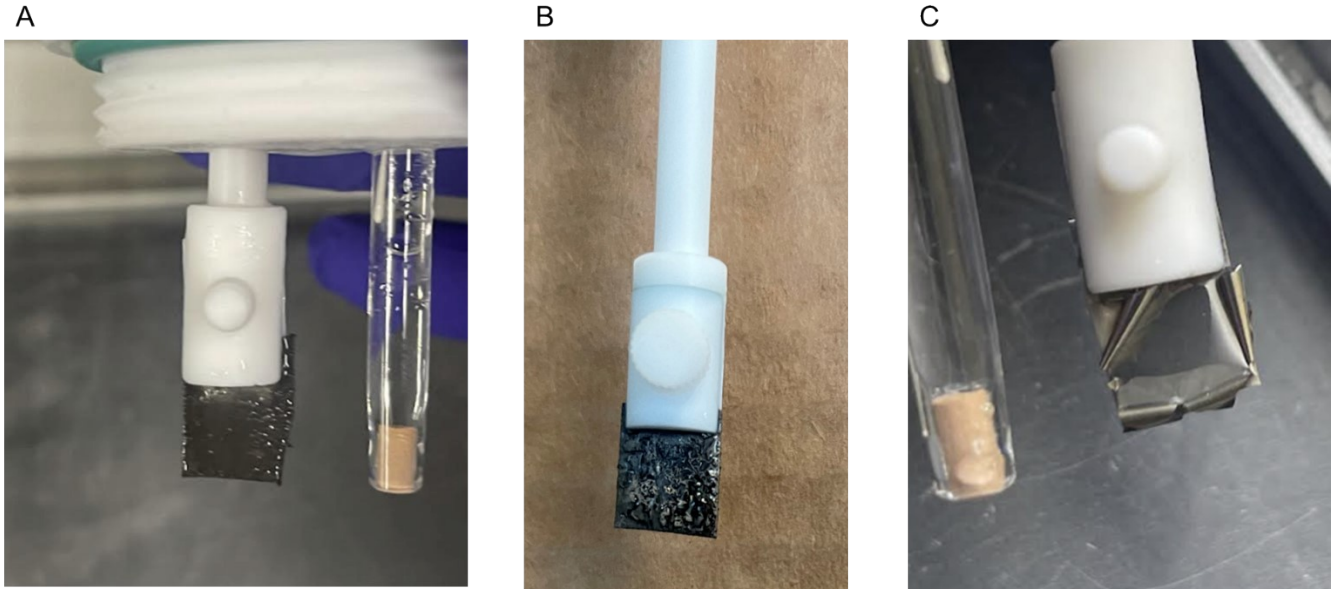

Fig. S.10: Snapshot of electrodes confirming successful nickel electrodeposition on the surface of the electrodes. **(a)** Electrodeposition in NH_4OH solvent at galvanostatic hold of 100 mA for 4 hours. **(b)** Electrodeposition in MEA solvent at galvanostatic hold of 100 mA for 4 hours. **(c)** Electrodeposition in NH_4OH solvent at potentiostatic hold of -0.45 V (vs RHE) for 2 hours.

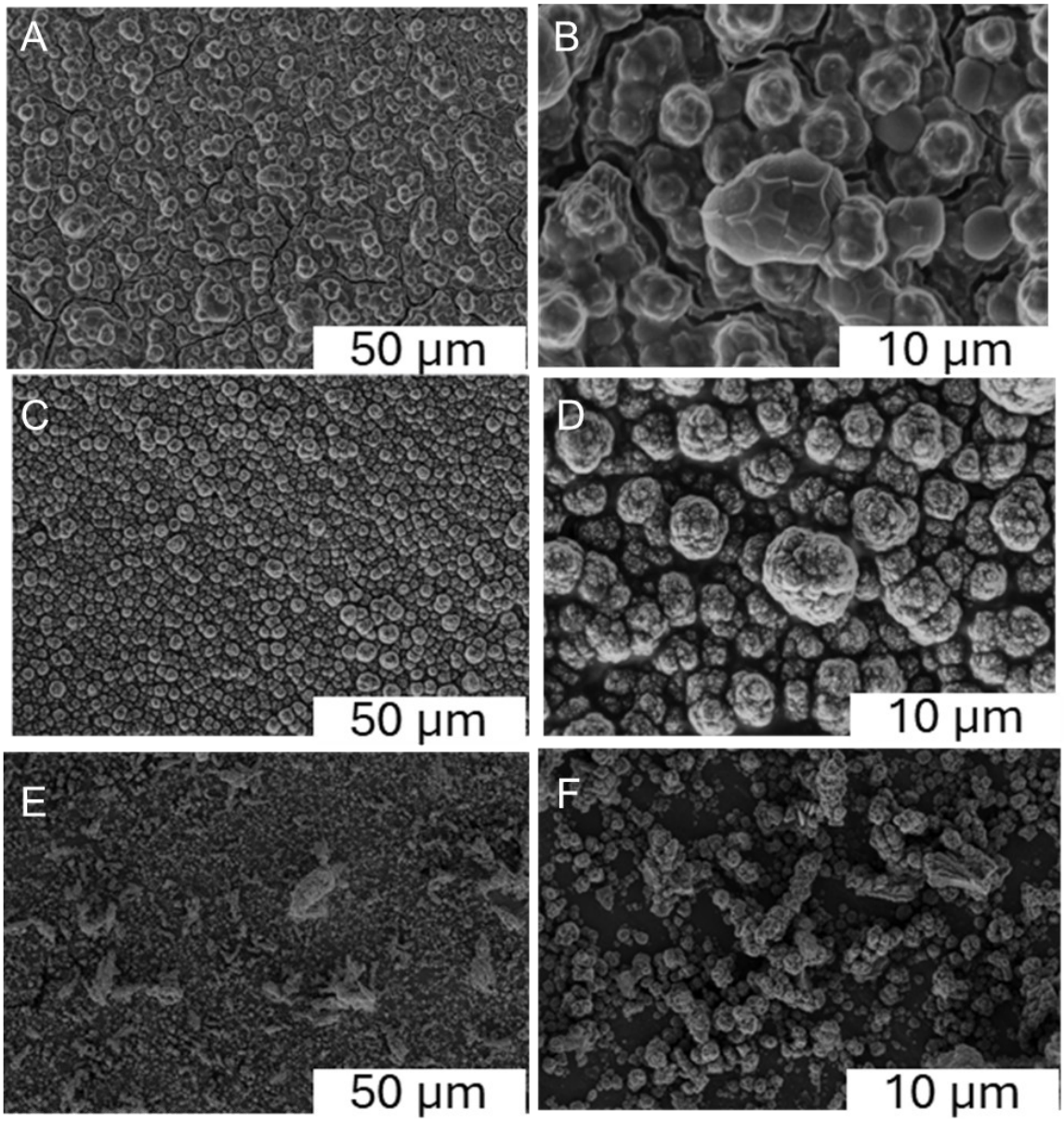

Fig. S.11. Morphologies of the electrodeposited nickel in NH_4OH, MEA, and DETA are evident in **(f)**, **(h)**, and **(j)** at a resolution of 50 µm, and in **(g)**, **(i)**, and **(k)** at a resolution of 10 µm, respectively. The anolyte used in all experiments is 0.25 M $NaNO_3$ solution and experiments are performed at room temperature.

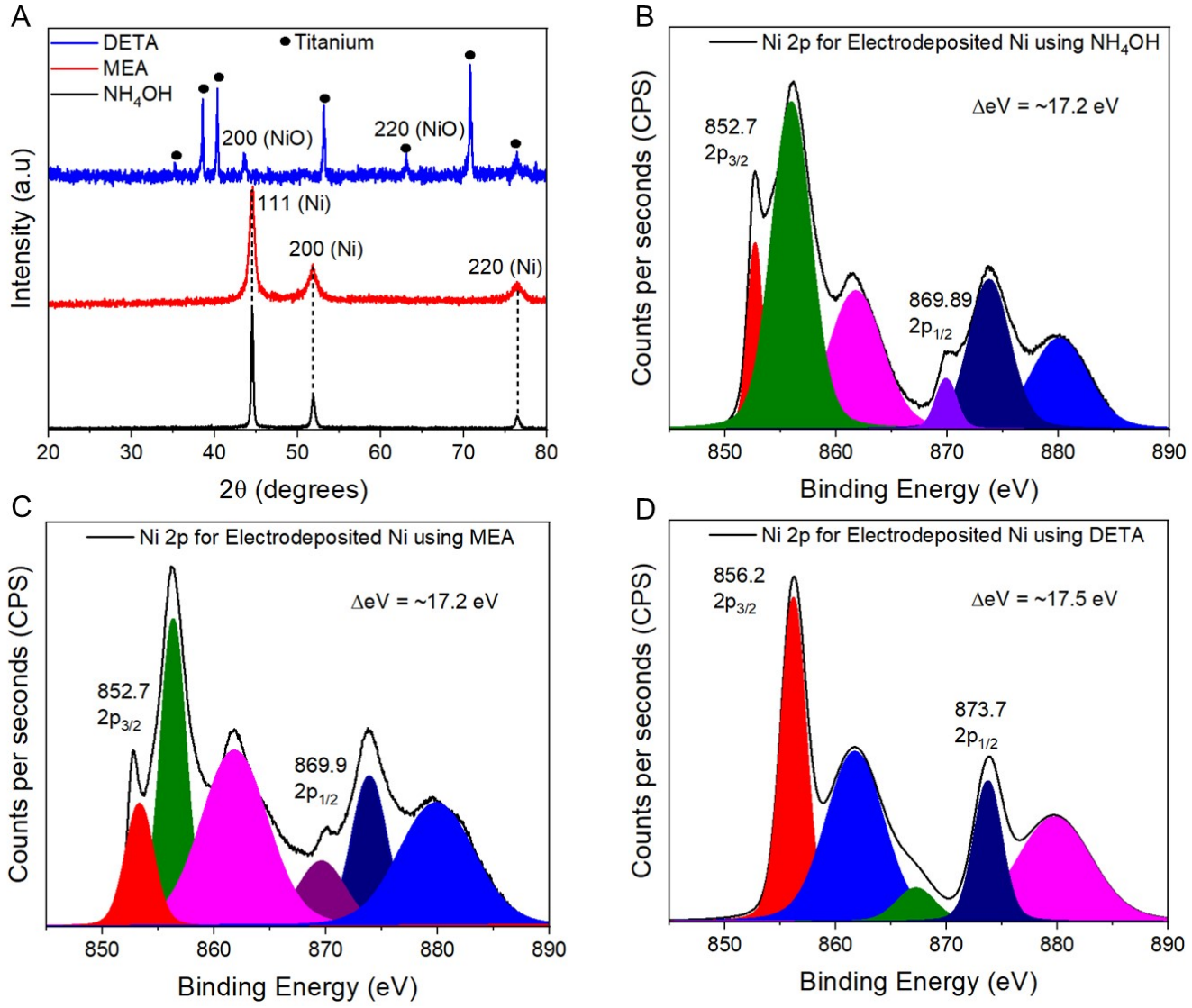

Fig S.12: Evidence of electrodeposited nickel from NH_4OH, MEA, and DETA with nickel bearing solutions is shown in **(a)**. High resolution scans for Ni 2p on electrodeposited nickel obtained from **(b)** NH_4OH, **(c)** MEA, and **(d)** DETA nickel bearing solutions using XPS.

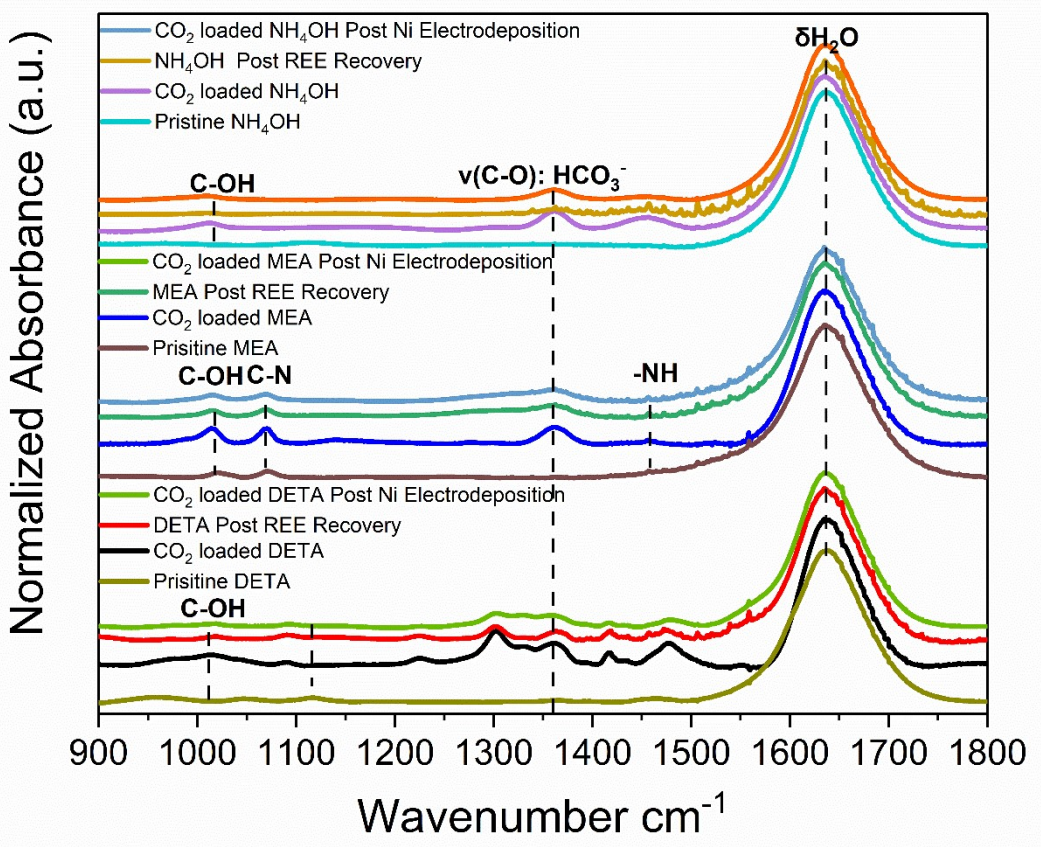

Fig. S.13: FTIR spectra showing the solvent transformations before CO_2 loading, after CO_2 loading, post REE extraction and post electrodeposition of Ni .

References

1. K.H. Gayer, L. Woonther , Hydrolysis of Cobalt Chloride and Nickel Chloride at 25°, 1952, **74**, 1436 -1437.
2. R. Cruz-Gaona, D. Dreisinger and C. Roel Cruz, In Electrochemistry in Mineral and Metal Processing VI: Proceedings of the International Symposium, 2003, **2003**, 304.
3. A. M. Fekry, *Electrochim Acta*, 2009, **54**, 3480–3489.
4. A. E. Martell and R. M. Smith, Critical Stability Constants Volume 4: Inorganic Complexes, Springer Science & Business Media, 2013.
5. A. E. Martell and R. M. Smith, Critical Stability Constants Volume 2: Amines, Springer Science & Business Media, 2012
6. A. E. Martell and R. M. Smith, Critical Stability Constants Volume 6: Second Supplement, Springer Science & Business Media, 2013.
7. A. E. Martell and R. M. Smith, Critical Stability Constants Volume 5: First Supplement, Springer Science & Business Media, 2013
8. M. Liu, A. Hohenshil and G. Gadikota, *Energy and Fuels*, 2021, **35**, 8051–8068.
9. B. Lv, B. Guo, Z. Zhou and G. Jing, *Environ Sci Technol*, 2015, **49**, 10728–10735.
10. B. Vallina, J. D. Rodriguez-Blanco, A. P. Brown, J. A. Blanco and L. G. Benning, *Nanoscale*, 2015, **7**, 12166–12179.
11. Y. Mao, B. Zhou and S. Peng, *Journal of Materials Science: Materials in Electronics*, 2020, **31**, 9457–9467.
12. M. S. Vidhya, G. Ravi, R. Yuvakkumar, D. Velauthapillai, M. Thambidurai, C. Dang and B. Saravanakumar, *RSC Adv*, 2020, **10**, 19410–19418.
13. G. J. Fan, A. G. H. Wee, R. Idem and P. Tontiwachwuthikul, *Ind Eng Chem Res*, 2009, **48**, 2717–2720.
14. A. Hartono, E. F. Da Silva, H. Grasdalen and H. F. Svendsen, *Ind Eng Chem Res*, 2007, **46**, 249–254.